Electron injection from mitochondrial transcription factor A to DNA associated with thymine dimer photo repair

AUTHOR(S):

Hashiya, Fumitaka; Ito, Shinji; Sugiyama, Hiroshi

CITATION:

Hashiya, Fumitaka ...[et al]. Electron injection from mitochondrial transcription factor A to DNA associated with thymine dimer photo repair. Bioorganic and Medicinal Chemistry 2019, 27(2): 278-284

ISSUE DATE:

2019-01-15

URL:

http://hdl.handle.net/2433/241651

Bioorganic & Medicinal Chemistry 27 (2019) 278–284

Contents lists available at ScienceDirect

Bioorganic & Medicinal Chemistry

journal homepage: www.elsevier.com/locate/bmc

Electron injection from mitochondrial transcription factor A to DNA associated with thymine dimer photo repair

Fumitaka Hashiya[a], Shinji Ito[c], Hiroshi Sugiyama[a,b,*]

[a] Department of Chemistry, Graduate School of Science, Kyoto University, Kitashirakawa-Oiwakecho, Sakyo, Kyoto 606-8502, Japan
[b] Institute for Integrated Cell-Material Sciences, Institute for Advanced Study, Kyoto University, Sakyo-ku, Kyoto 606-8501, Japan
[c] Medical Research Support Center, Graduate School of Medicine, Kyoto University, Sakyo-ku, Kyoto 606-8501, Japan

ARTICLE INFO

Keywords:
Bromouracil
Electron transfer
Photochemical
Mitochondria
TFAM

ABSTRACT

Electron transfer through π-stacked arrays of double-stranded DNA contributes to the redox chemistry of bases, including guanine oxidation and thymine–thymine dimer repair by photolyase. 5-Bromouracil is an attractive photoreactive thymine analogue that can be used to investigate electron transfer in DNA, and is a useful probe for protein–DNA interaction analysis. In the present study using ^{Br}U we found that UV irradiation facilitated electron injection from mitochondrial transcription factor A into DNA. We also observed that this electron injection could lead to repair of a thymine–thymine dimer.

1. Introduction

A charge transfer through π-stacked arrays of double-stranded DNA contribute to critical redox chemistry for DNA. For example, a positive charge transfer promotes oxidative damage to guanine in DNA, which possibly relates to the presence of mutation hot spots in the genome.[1–4] It has also been reported that an electron transfer from $FADH^-$ through tryptophan residues is crucial for DNA repair involving thymine–thymine dimer photo repair by photolyase.[5,6] 5-Bromouracil (^{Br}U) is an attractive photoreactive thymine analogue that can be used to investigate electron transfer in dsDNA: because electron transfer within DNA generates a reactive 5-yl-uracil radical from ^{Br}U, such an electron transfer can be detected by the consequent reaction product. Replacement of thymine in DNA with ^{Br}U results in retention of almost all the functional properties of DNA, even in living cells. Hence, ^{Br}U has also been used to evaluate protein–DNA interactions.[7–15] Using ^{Br}U we previously demonstrated electron transfer from the archaeal DNA-binding protein sso7d to DNA and showed that this electron transfer repaired thymine–thymine dimers in a similar fashion to photolyase.[16,17]

Mitochondrial transcription factor A (TFAM) is a DNA-binding protein comprising a tandem high-mobility group (HMG) box domain and a short C-terminal tail; it plays a critical role during transcription, replication, and maintenance of the mitochondrial genome. The mammalian mitochondrial genome contains three promoters: light-strand promoter (LSP), heavy-strand promoter 1 (HSP1), and heavy-strand promoter 2 (HSP2), which drive mitochondrial DNA (mtDNA) transcription. Because truncated RNA transcripts from LSP initiate mtDNA replication, TFAM is also an essential factor for replication; thus, knockout of TFAM is embryonic lethal[18,19] and knockdown leads to a decreased copy number of mtDNA.[20] TFAM also contributes to form nucleoids, which resemble the nucleosome in eukaryotes. Ngo and coworkers reported the crystal structures of TFAM binding to LSP, HSP1, and non-sequence-specific DNA in which DNA was constrained into a U-shape to allow compaction and stabilization of mtDNA.[21,22] Approximately 1000 molecules of TFAM are present per mtDNA molecule, which is enough to cover the entire length of mtDNA given that TFAM occupies about 25 bp.[23]

In the present study, we focused on tyrosine and tryptophan residues located in the DNA-binding site of human TFAM that were sufficiently close together to cause long-range electron transfer for thymine residues which can be replaced with ^{Br}U, and demonstrated electron injection from TFAM into DNA using a ^{Br}U probe. TFAM bound to DNA not only through the strongly positioning sequence in LSP or HSP1, but also in a non-sequence-specific manner, and injected electrons into the DNA. We also demonstrated that the electron injection facilitated photo repair of thymine–thymine dimers.

* Corresponding author at: Department of Chemistry, Graduate School of Science, Kyoto University, Kitashirakawa-Oiwakecho, Sakyo, Kyoto 606-8502, Japan.
E-mail address: hs@kuchem.kyoto-u.ac.jp (H. Sugiyama).

https://doi.org/10.1016/j.bmc.2018.11.044
Received 5 November 2018; Received in revised form 28 November 2018; Accepted 29 November 2018
Available online 29 November 2018

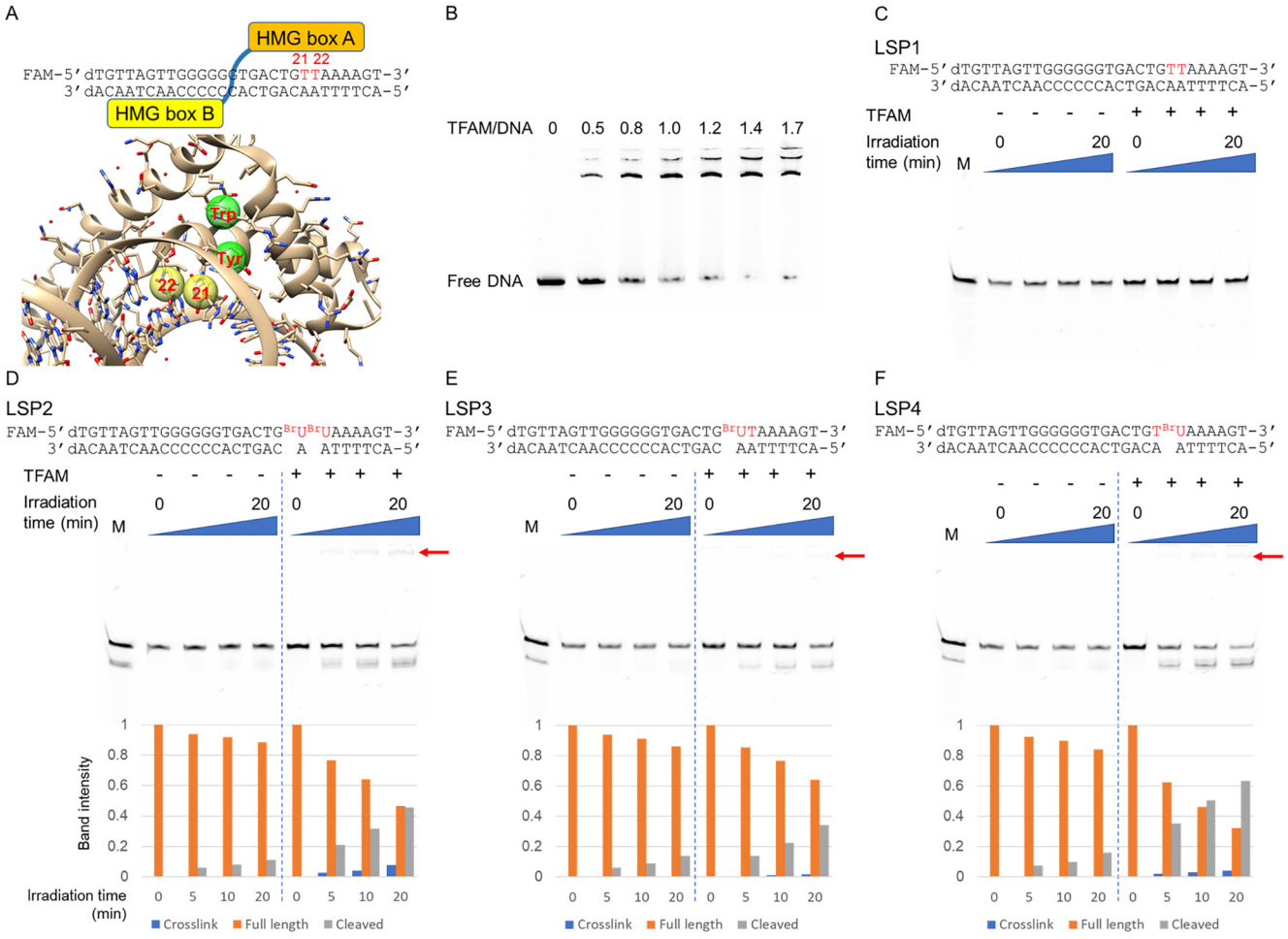

Figure 1. Photoirradiation for TFAM–LSP complex. (A) Schematic of TFAM binding by LSP1 and crystal structure around thymine 21, thymine 22, tyrosine, and tryptophan residues in the HMG box A domain. (B) EMSA of TFAM–LSP1 complex. (C, D, E and F) Results of denaturing PAGE analysis locating uracil residues in LSP1, 2, 3, and 4, respectively. These samples were irradiated at 302 nm for 0, 5, 10, and 20 min in the absence or presence of TFAM. Ladders prepared by treating each LSP fragment with piperidine and heat were applied in lane M to indicate ^{Br}U-substituted sites. The red arrow indicates a band resulting from TFAM–LSP crosslinking. Bar charts at the bottom of D, E, and F represent the percentage band intensities for crosslinked, full-length, and cleaved TFAM–LSP.

2. Material and methods

2.1. Preparation of recombinant TFAM

The human TFAM cDNA was prepared by PrimeScript RT reagent Kit (TaKaRa). PCR was carried out with primer 1 and 2 (Supplementary Table 1) to connect *Nde*I and *Xho*I sites using KOD plus Neo (Toyobo). The product which encodes residues 43–246, corresponding to full length TFAM after cleavage of the *N*-terminal mitochondrial leader sequence was inserted into pET28a expression vector. The sequence confirmed TFAM expression plasmid was transformed into BL21(DE3). Single colony was incubated with 500 ml of auto-inducer medium, LB medium containing 2 g/l lactose, 400 mg/l glucose and 150 mg/l $MgSO_4$, containing 50 μg/l kanamycin at 37 °C for 15 h. The cells were harvested and resuspended with resuspend buffer (20 mM Tris-HCl, 100 mM NaCl, 20 mM imidazole, 1 mM benzamidine, 1 mM 2-mercaptoethanol, pH 7.5). The resuspended solution was incubated with 10 units/ml benzonase nuclease (SIGMA-ALDRICH) and 1 mg/ml lysozyme (Nacalai) at 4 °C for 1 h and subsequently sonicated for 5 min (10 *sec* on and 20 *sec* off) on ice. After centrifugation, the supernatant was purified by affinity chromatography using HisTrap FF (GE healthcare) on AKTA pure 25 protein purification system (GE healthcare) with elution buffer (20 mM Tris-HCl, 500 mM NaCl, 40–400 mM imidazole, 1 mM benzamidine, 1 mM 2-mercaptoethanol, pH 7.5). The fractions containing His-tagged TFAM were subsequently purified by gel filtration chromatography using Superdex 200 Inclease 10/300 GL (GE healthcare) with gel filtration buffer (20 mM Tris-HCl, 300 mM NaCl, 1 mM 2-mercaptoethanol, pH 7.5). The fractions containing His-tagged TFAM were concentrated by Amicon Ultra 4 (Merck) which cutoff molecular weight bellow 10 kDa and stored at 4 °C or −80 °C for long term. The concentration of recombinant TFAM was measured by Qubit 4 Fluorometer (ThermoFisher).

2.2. Preparation of DNA fragments

FAM labelled LSP top 1–4 and HSP top 1–4 DNA fragments were purchased from Japan Bio Services. The complementary strands for the fragments, LSP bottom or HSP bottom, were purchased from SIGMA-ALDRICH. Thymine dimer containing DNA fragment, LSP top T < > T, was purchased from Tsukuba Oligo Service. Each top strand and its complementary bottom strand were mixed in irradiation buffer (10 mM sodium cacodylate, 10 mM NaCl, pH 7.0) and incubated at 95 °C for 5 min. After the incubation the temperature was gradually decreased to form double stranded LSP or HSP. Non-sequence specific DNA was prepared by conventional PCR amplification with 601 core sequence as a template, primer 3 and Texas Red labeled primer 4 except that d^{Br}UTP was used instead of dTTP. The sequences of each DNA oligo are shown in Supplementary Table 1. 601 core sequence is as follows:

5′dTGGAGAATCCCGGTGCCGAGGCCGCTCAATTGGTGTAGCAAGC
TCTAGCACCGCTTAAACGCACGTACGCGCTGTCCCCCGCGTTTTAACC

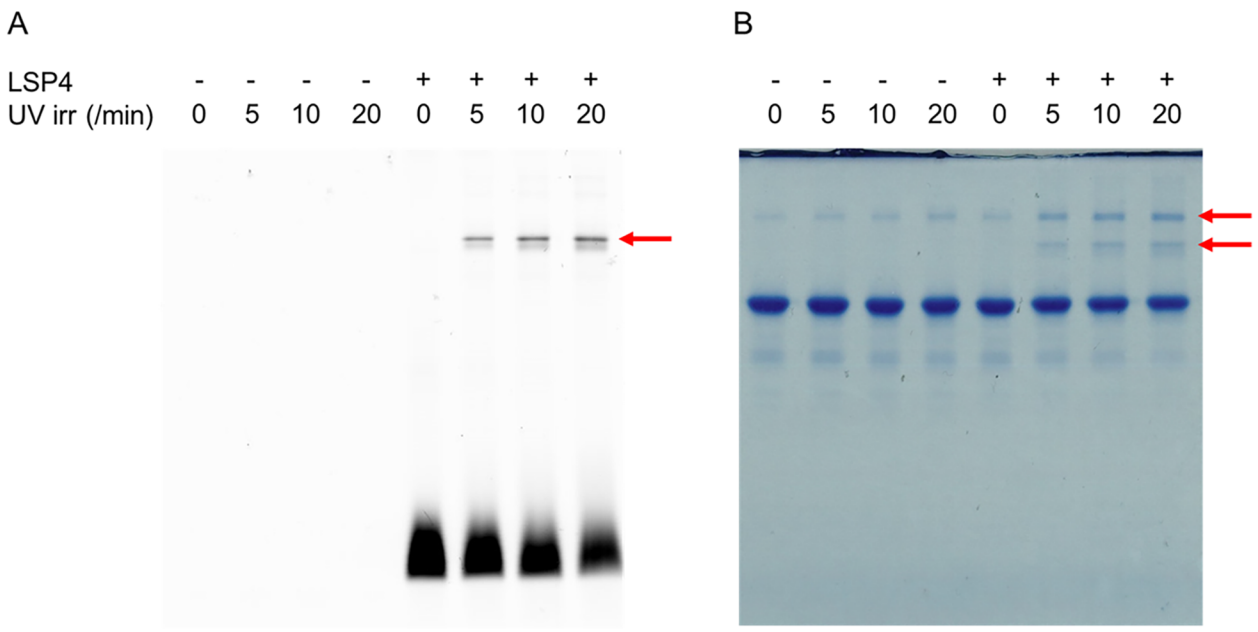

Figure 2. SDS–PAGE analysis of photoirradiation for TFAM–LSP4 complex. The samples were irradiated at 302 nm for 0, 5, 10, and 20 min in the absence or presence of LSP4. (A) Fluorescence image of SDS–PAGE. A red arrow indicates the TFAM–LSP4 crosslinked product. (B) Coomassie Brilliant Blue-stained SDS–PAGE. The upper and lower bands indicated by red arrows resulted from crosslinked TFAM–TFAM and TFAM–LSP4 products, respectively.

GCCAAGGGGATTACTCCCTAGTTCCAGGCACGTGTCAGATATATACAT CCTGT-3′

2.3. Photoirradiation and denaturing polyacrylamide gel electrophoresis (PAGE) assay for LSP or HSP

1 μM LSP or HSP DNA fragment was dissolved in irradiation buffer in the absence or in the presence of 1.4 μM TFAM and incubated for 30 min at room temperature. The volume of each samples was 40 μl. Photoirradiation was performed under aerobic condition using a 3UV^{TM} Transilluminator (UVP) for 302 nm irradiation or a HM-3 hyper monochromatic light source (JASCO) for 280, 300 and 310 nm monochromatic irradiation. After the irradiation, 5 μl of 10x uracil DNA glycosylase (UDG) buffer, 5 U of UDG (NEW ENGLAND BioLabs) and 5 μl of Milli Q water were added for each samples and incubated at 37 °C for 60 min for locating uracil residues or 5 μl of 10x pyrimidine dimer glycosylase (PDG) buffer, 20 U of PDG (NEW ENGLAND BioLabs), 0.5 μl of 100x BSA and 4.5 μl of Milli Q water were added and incubated at 37 °C for 180 min for locating thymine dimer. Finally, all reaction mixtures were dried up using vacuum, dissolved in 40 μl of Loading Dye (prepared from 300 μl of EDAT, 200 μl of Milli Q water and 10 ml of formamide colored with New fuchsin) and heated at 95 °C for 5 min. Mini slab gel filled with denaturing polyacrylamide gel (8 M urea, 20% polyacrylamide, 1x TBE buffer, pH 8.3) was used to detect DNA cleavages. Each LSP or HSP fragments treated with piperidine and heat which produced cleavage on 5-halopyrimidine site, in this case ^{Br}U, were applied as ladder in the PAGE assay.

2.4. Photoirradiation and slab gel sequencing assay for non-sequence specific DNA

100 nM non-sequence specific DNA fragment was dissolved in irradiation buffer in the absence or in the presence of 600 nM TFAM and incubated for 30 min at room temperature. The volume of each samples was 15 μl. Photoirradiation was performed under aerobic condition using a 3UV^{TM} Transilluminator (UVP) for 302 nm irradiation. After the irradiation, 3 μl of 10x UDG buffer, 5 U of UDG and 12 μl of Milli Q water were added for each samples and incubated at 37 °C for 60 min. Finally, all reaction mixtures were dried up using vacuum, dissolved in 15 μl of Loading Dye and heated at 95 °C for 5 min. DNA sequence ladder was prepared from Texas Red labeled primer 4 using Thermo Sequenase Dye Primer Manual Cycle Sequencing Kit. Photo irradiated samples dissolved in Loading Dye were analyzed with sequence ladder by SQ5500E (HITACHI) slab gel sequencer filled with denaturing polyacrylamide gel (6 M urea, 6% polyacrylamide, 1x TBE buffer, pH 8.3) to detect DNA cleavages.

2.5. Tryptic digestion and LC/MS/MS

1.4 μM TFAM was dissolved in irradiation buffer in the absence or in the presence of 1 μM LSP4 and incubated for 30 min at room temperature. Photoirradiation was performed under aerobic condition using a 3UV^{TM} Transilluminator (UVP). After drying up using vacuum, all samples were dissolved in SDS sample buffer (30 mM Tris-HCl, 1% SDS, 2.5% sucrose, 50 mM 2-mercaptoethanol, pH 6.8) and heated at 95 °C for 5 min. SDS-PAGE was carried out to separate each products and In-Gel Tryptic Digestion Kit (ThermoFisher) was used to obtain peptide fragments. Tryptic digestion samples were analyzed using TripleTOF5600 + (SCIEX).

3. Results

3.1. Electron injection into LSP or HSP

A TFAM–DNA complex comprising recombinant human TFAM and a 28-bp DNA fragment derived from LSP was used for the photoirradiation experiment. Four LSP variants (LSP1–4) were prepared by replacing thymines 21 or 22, which are close to the HMG box A in TFAM, with ^{Br}U. According to the crystal structure of the TFAM–LSP complex (PDB ID: 3TMM), the distances between thymines 21 and 22 and the proximate aromatic amino acid, Tyr57, are 5.87 and 8.36 Å, respectively. This is close enough to cause long-range electron transfer (Fig. 1A). The binding affinity for an LSP1 that did not contain ^{Br}U was evaluated by electrophoretic mobility shift assay (EMSA). The decrease in the amount of free LSP reached a plateau at 1.0 eq TFAM (Fig. 1B). The TFAM-binding affinity of an LSP2 in which both thymines 21 and 22 were replaced with ^{Br}U was almost identical to that of LSP1, suggesting that ^{Br}U replacement did not affect the binding affinity (Fig. S1).

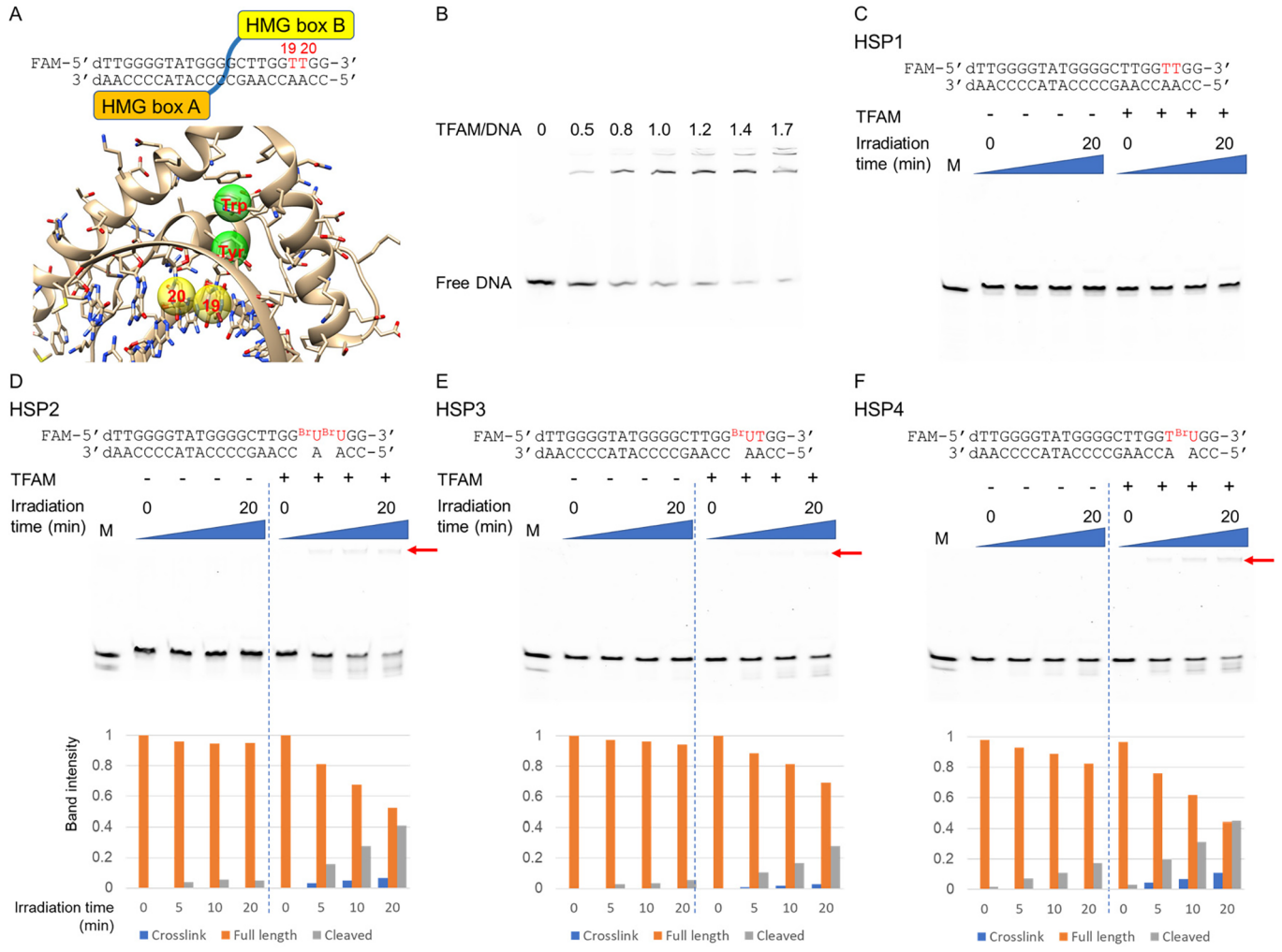

Figure 3. Photoirradiation of TFAM–HSP complex. (A) Schematic of TFAM binding to HSP and the crystal structure around thymine 19, thymine 20, tyrosine, and tryptophan residues in the HMG box B domain. (B) EMSA of TFAM–HSP1 complex. (C, D, E, and F) Results of denaturing PAGE analysis locating uracil residues in HSP1, 2, 3, and 4, respectively. These samples were irradiated at 302 nm for 0, 5, 10, and 20 min in the absence or presence of TFAM. Ladders prepared by treating each HSP fragment with piperidine and heat were applied in lane M. The red arrow indicates a band resulting from a TFAM–HSP crosslinked product. Bar charts at the bottom of D, E, and F represent the percentage band intensities for crosslinked, full-length, and cleaved TFAM–HSP.

As described previously, photoirradiation at 302 nm and subsequent treatment with heat and uracil–DNA glycosylase (UDG) selectively produced DNA cleavage at uracil sites generated from ^{Br}U by electron transfer (24). Incidentally, these DNA cleavages were not produced in the absence of UDG (Fig. S2). Denaturing polyacrylamide gel electrophoresis (PAGE) assay demonstrated that photoirradiation of an LSP1 fragment that did not contain ^{Br}U did not produce cleavage in either the absence or presence of TFAM (Fig. 1C). In contrast, photoirradiation of LSP2, LSP3, and LSP4 in the presence of TFAM led to dramatic DNA cleavage at the locations of the uracil residues generated by electron transfer, whereas little DNA cleavage was observed in the absence of TFAM (Fig. 1D, E, and F). Photoirradiation also produced an upper band shift in the presence of TFAM that resulted from a TFAM–DNA crosslink. According to the intensity analysis of all bands resulting from crosslinked, full-length, and cleaved products, LSP4, which possesses a ^{Br}U at position 22, showed a higher efficiency of DNA cleavage than LSP3, which possesses a ^{Br}U at position 21. This suggested that a ^{Br}U at position 22 more effectively generated uracil radicals.

Further analysis of the TFAM–LSP4 crosslinked product was carried out by SDS–PAGE. On a fluorescence image, DNA band shifts were observed with increasing photoirradiation time, which is consistent with the results of denaturing PAGE (Fig. 2A). Photoirradiation in the presence of LSP4 led to the appearance of two protein bands in the Coomassie Brilliant Blue-stained image (Fig. 2B). The retardation of a lower band matched the shifted band in the fluorescence image. LS/MS/MS analysis revealed that both an upper and a lower band contained peptide fragments derived from TFAM; therefore, the lower band contained a TFAM–LSP4 crosslinked product and the upper band possibly contained covalently crosslinked TFAM proteins.

Similar photoirradiation experiments were carried out using another TFAM–DNA complex comprised of TFAM and a 22-bp DNA fragment derived from HSP1. Four variants of HSP were prepared by replacing thymines 19 or 20, which are close to the HMG box B in TFAM. According to the crystal structure of the TFAM–HSP1 complex (PDB ID: 4NOD), the distances between thymines 19 and 20 and the proximate aromatic amino acid, Tyr162, are 6.91 and 8.08 Å, respectively (Fig. 3A). The binding affinity of HSP differed slightly from that of LSP. The decrease in the amount of free HSP reached a plateau at 0.8 eq of TFAM whereas that of LSP reached a plateau at 1.0 eq (Fig. 3B) and the ^{Br}U replacement did not affect the TFAM-binding affinity for HSP (Fig. S3). The photoirradiation for these TFAM–HSP complexes gave similar results to those obtained with the TFAM–LSP complex (Fig. 3C, D, E, and F). It is noteworthy that HSP4, which possesses a ^{Br}U at position 20, showed higher photoreactivity than HSP3, which possesses a ^{Br}U at position 19. This suggested that a 3′ ^{Br}U was more photoreactive than a 5′ ^{Br}U in photoirradiation of both LSP and HSP,

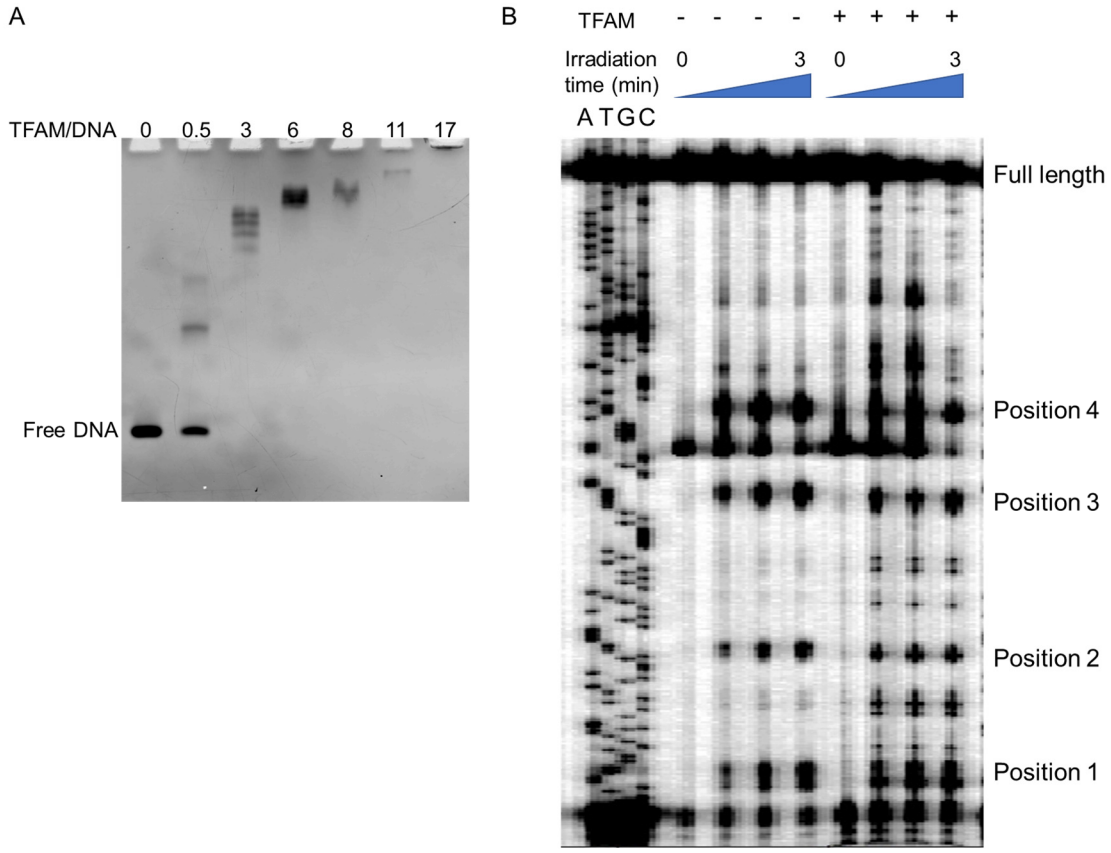

Figure 4. Photoirradiation of a TFAM–non-sequence-specific DNA complex. (A) EMSA of TFAM-binding affinity for the 601 sequence. (B) Result of slab gel sequencer analysis for locating uracil residues in the 601 sequence. These samples were irradiated for 0, 1, 2, and 3 min.

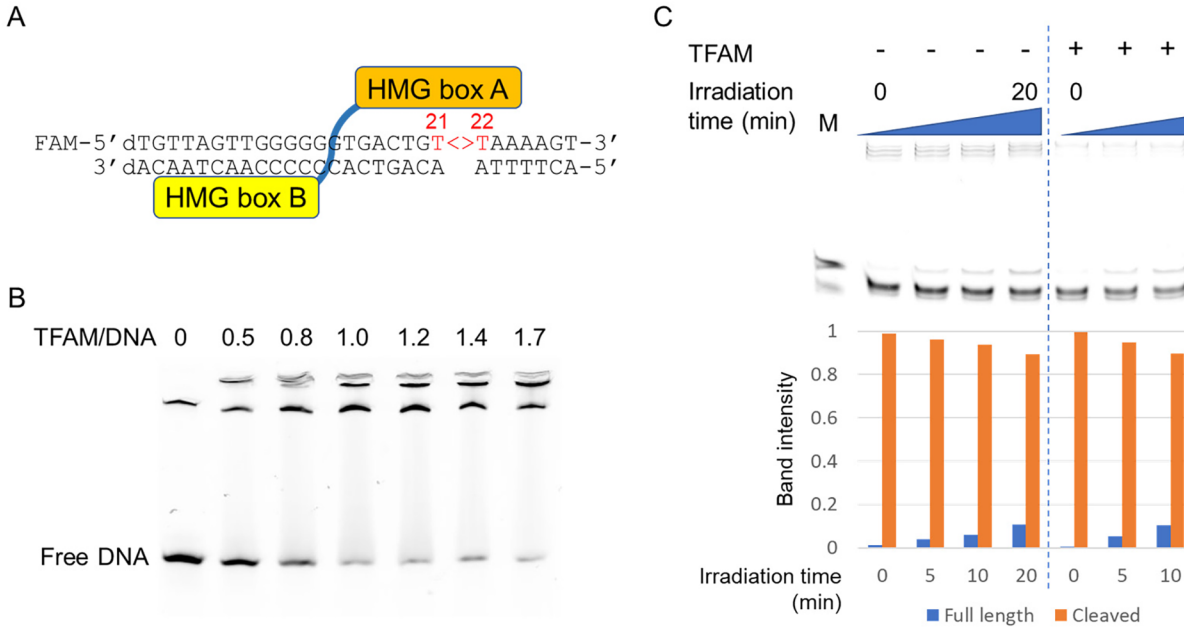

Figure 5. Thymine dimer photo repair in TFAM–LSP-T < > T complex. (A) Schematic of LSP-T < > T. (B) EMSA of TFAM–LSP-T < > T complex. (C) Result of denaturing PAGE analysis of LSP-T < > T after photoirradiation and PDG treatment in the absence or presence of TFAM. The samples were irradiated for 0, 5, 10, and 20 min. Ladders prepared by treating LSP2 fragments with piperidine and heat were applied in lane M to indicate thymines 21 and 22. The bar chart at the bottom of C represents the percentage band intensities for full-length and cleaved fragments.

even though the 3′ ^{Br}U is more distant from the proximate tyrosine than the 5′ ^{Br}U. Previously, we examined the photoreactivity of ^{Br}U-substituted DNA and reported that uracil radicals were effectively generated in certain sequences: 5′/3′-G/C[*A*]$_{n=1,\ 2,\ 3}$ ^{Br}U^{Br}U-3′/5′. We termed this a "hot-spot sequence". In ^{Br}U-substituted DNA, photoirradiation of the hot-spot sequence facilitates electron transfer from G and the electron is trapped by ^{Br}U^{Br}U to form anion radical [^{Br}U^{Br}U]$^{\bullet-}$. Subsequent release of a Br^- generates the uracil-5-yl radical[24,25]. We

performed photoirradiation of the self-complementary hot-spot sequence 5′-CGAA^{Br}U^{Br}UCG-3′ and 5′-GC^{Br}U^{Br}UAAGC-3′. HPLC analysis revealed that an uracil residue was effectively generated from a 3' ^{Br}U rather than 5' in both hot-spot sequences[24]. These results suggest that a 3' ^{Br}U is more photoreactive than 5' in [^{Br}U^{Br}U]$^{\bullet-}$ and releases Br^- effectively to generate uracil radical. Consistent with the results, a 3' ^{Br}U in both LSP and HSP effectively generated uracil radical in the present study.

3.2. Electron injection into nonspecific DNA

In addition to the strongly positioning sequences in LSP and HSP1, it has been reported that TFAM interacts nonspecifically with DNA to compact it. To evaluate the electron transfer to a non-sequence-specific DNA, a 147-bp DNA fragment in which all thymine residues were substituted with ^{Br}U was prepared from the 601 nucleosome strongly positioning sequence, which is not related to mitochondria. The binding affinity of TFAM for this DNA fragment was evaluated by EMSA (Fig. 4A). An excess of more than 6 eq TFAM produced aggregation and decreased the DNA band intensity. Given that the DNA fragment was 5.2-fold longer than LSP, it is possible that 6 eq TFAM most effectively formed a complex with DNA. Consistent with previous results, photoirradiation of the non-sequence-specific DNA produced cleavage at hot-spot sequences denoted at positions 1–4 in both the absence and presence of TFAM (Fig. 4B). Besides such background cleavage, TFAM enhanced the photosensitivity of the DNA and produced new DNA cleavage mainly at ^{Br}U-substituted sites. These results suggest that TFAM can bind to DNA in a non-sequence-specific manner and cause electron transfer.

3.3. Thymine-thymine dimer photo-restoration

Photolyase catalyzes electron transfer from $FADH^-$ to DNA through its tryptophan residues to repair thymine–thymine dimers, a common UV-induced DNA lesion[5,6]. In addition, facilitation by photoirradiation of electron transfer from an aromatic amino acid residue, especially tryptophan or tyrosine, to DNA repairs the thymine–thymine dimer[16,17,26,27]. Because we had demonstrated electron transfer from TFAM, we evaluated the photo repair of thymine–thymine dimers by electron transfer. A DNA fragment LSP-T < > T, in which thymines 21 and 22 formed a thymine–cyclobutane dimer, was prepared and used to generate a TFAM–LSP-T < > T complex (Fig. 5A). The binding affinity of TFAM for LSP-T < > T as evaluated by EMSA was identical with that of LSP1 (Fig. 5B). Although LSP-T < > T was completely digested by pyrimidine dimer glycosylase (PDG) without 302-nm photoirradiation, photoirradiation led to moderate levels of repair of the thymine–thymine dimer, and a full-length LSP was detected in denaturing PAGE analysis. According to a band-intensity analysis, the efficiency of thymine–thymine dimer repair in the presence of TFAM was 2-fold higher than in its absence. Consistent with this result, thymine dimer repair in monochromatic UV light irradiation at 300 nm or 310 nm was enhanced in the presence of TFAM (Fig. S4).

4. Discussion

A prokaryotic DNA packing protein, HU, which like TFAM constrains DNA into a U-shape, preferentially interacts with damaged DNA, for example at a base-pair mismatch or base flip out, and recruits damage-repair enzymes[28]. TFAM also preferentially interacts with cisplatin-damaged DNA and oxidized DNA[29]. In the present study, we detected no binding preference of TFAM for intact DNA over damaged DNA containing thymine–thymine dimers. However, there is sufficient TFAM in mitochondria to cover the entire mtDNA and allow damaged base pairs to interact with TFAM. TFAM could interact not only with strongly positioning sequences on LSP and HSP, but also with a non-sequence-specific DNA, causing electron transfer into DNA during photoirradiation. Further, this electron transfer facilitated photo repair of thymine–thymine dimers.

mtDNA is physiologically vulnerable because of the mitochondrial respiratory chain that generates reactive oxygen species (ROS), and may therefore accumulate more oxidative DNA damage than nuclear DNA. It is known that oxidative DNA damage in mitochondria is repaired by base excision repair (BER).[30] However, the possibility of repair of thymine–thymine dimers in mtDNA by BER has been discounted by radioisotope-labeled thymidine incorporation experiments, although the accumulation of thymine–thymine dimers depletes mtDNA.[31] TFAM contributes to mtDNA replication because the truncated RNA transcripts from LSP become a primer to initiate mtDNA replication, and knockdown of TFAM leads to depletion of mtDNA and mitochondrial dysfunction. However, given that expression of human TFAM, which does not work as a transcription factor in mouse cells, increases the amount of mtDNA in mouse cells[32] and that the transcription level does not correlate with the amount of mtDNA,[20] TFAM itself may act as an essential factor for mtDNA stabilization rather than as a replication factor. We hypothesize that TFAM contributes to repair of thymine–thymine dimers by electron transfer and thereby maintains mtDNA.

5. Conclusion

Using ^{Br}U as a probe, we demonstrated electron transfer from TFAM to DNA that was facilitated by photoirradiation. TFAM effectively interacted with not only strongly positioning sequences in LSP and HSP1 but with a non-sequence-specific DNA fragment to cause electron transfer. The binding affinity of TFAM for intact DNA and damaged DNA containing thymine dimers was identical and the electron transfer from TFAM enhanced thymine dimer photo repair. The contribution of TFAM to mtDNA maintenance remains elusive and the present results may provide an important insight into mtDNA stabilization by TFAM.

Funding

This work was supported by Grant-in-Aid for JSPS Research Fellow Grant Number 16J03092 and JSPS KAKENHI Grant Number JP16H06356.

Appendix A. Supplementary data

Supplementary data to this article can be found online at https://doi.org/10.1016/j.bmc.2018.11.044.

References

1. Rogozin IB, Pavlov YI. Theoretical analysis of mutation hotspots and their DNA sequence context specificity. *Mutat Res Mutat Res.* 2003;544(1):65–85. https://doi.org/10.1016/S1383-5742(03)00032-2.
2. Delaney S, Barton JK. Long-range DNA charge transport. *J Org Chem.* 2003;68(17):6475–6483. https://doi.org/10.1021/jo030095y.
3. Hall DB, Holmlin RE, Barton JK. Oxidative DNA damage through long-range electron transfer. *Nature.* 1996;382:731–735.
4. Giese B. Long-distance charge transport in DNA: the hopping mechanism. *Acc Chem Res.* 2000;33(9):631–636. https://doi.org/10.1021/ar990040b.
5. Carell T, Burgdorf LT, Kundu LM, Cichon M. The mechanism of action of DNA photolyases. *Curr Opin Chem Biol.* 2001;5(5):491–498. https://doi.org/10.1016/S1367-5931(00)00239-8.
6. Sancar A. Structure and Function of DNA Photolyase. *Biochemistry.* 1994;33(1):2–9. https://doi.org/10.1016/0925-8388(94)90852-4.
7. Sugiyama H, Tsutsumi Y, Saito I. Highly Sequence Selective Photoreaction of 5-Bromouracil-Containing Deoxyhexanucleotides. *J Am Chem Soc.* 1990;112(18):6720–6721. https://doi.org/10.1021/ja00174a046.
8. Hicke BJ, Cech TR, Willis MC, Koch TH. Telomeric Protein-DNA Point Contacts Identified by Photo-Cross-Linking Using 5-Bromodeoxyuridine. *Biochemistry.* 1994;33(11):3364–3373. https://doi.org/10.1021/bi00177a030.
9. Sugiyama H, Fujimoto K, Saito I. Preferential C1' hydrogen abstraction by a uracil radical in a DNA-RNA hybrid. *Tetrahedron Lett.* 1997;38(46):8057–8060.
10. Oyoshi T, Kawai K, Sugiyama H. Efficient C2'α-hydroxylation of deoxyribose in protein-induced Z-form DNA. *J Am Chem Soc.* 2003;125(6):1526–1531. https://doi.org/10.1021/ja028388g.

11. Xu Y, Ikeda R, Sugiyama H. 8-Methylguanosine: A Powerful Z-DNA Stabilizer. *J Am Chem Soc.* 2003;125(44):13519–13524. https://doi.org/10.1021/ja036233i.
12. Tashiro R, Sugiyama H. Unique charge transfer properties of the four-base π -stacks in Z-DNA. *J Am Chem Soc.* 2003;125:15282–15283.
13. Xu Y, Sugiyama H. Highly efficient photochemical 2′-deoxyribonolactone formation at the diagonal loop of a 5-iodouracil-containing antiparallel G-quartet. *J Am Chem Soc.* 2004;126(20):6274–6279. https://doi.org/10.1021/ja031942h.
14. Willis MC, Hicke BJ, Uhlenbeck OC, Cech TR, Koch TH. Photocrosslinking of 5-iodouracil-substituted RNA and DNA to proteins. Science (80-). 1993;262(5137):1255–1257. doi:10.1126/science.7694369.
15. Saha A, Kizaki S, De D, Endo M, Kim KK, Sugiyama H. Examining cooperative binding of Sox2 on DC5 regulatory element upon complex formation with Pax6 through excess electron transfer assay. *Nucleic Acids Res.* 2016;44(14):e125https://doi.org/10.1093/nar/gkw478.
16. Oyoshi T, Wang AHJ, Sugiyama H. Photoreactivity of 5-Iodouracil-containing DNA-Sso7d complex in solution: the protein-induced DNA kink causes intrastrand hydrogen abstraction from the 5-methyl of thymine at the 5' side. *J Am Chem Soc.* 2002;124(10):2086–2087. https://doi.org/10.1021/ja016968s.
17. Tashiro R, Wang AH-J, Sugiyama H. Photoreactivation of DNA by an archaeal nucleoprotein Sso7d. Proc Natl Acad Sci USA. 2006;103(45):16655–16659. doi:10.1073/pnas.0603484103.
18. Falkenberg M, Larsson N-G, Gustafsson CM. DNA Replication and Transcription in Mammalian Mitochondria. *Annu Rev Biochem.* 2007;76(1):679–699. https://doi.org/10.1146/annurev.biochem.76.060305.152028.
19. Bonawitz ND, Clayton DA, Shadel GS. Initiation and Beyond: Multiple Functions of the Human Mitochondrial Transcription Machinery. *Mol Cell.* 2006;24(6):813–825. https://doi.org/10.1016/j.molcel.2006.11.024.
20. Kanki T, Ohgaki K. Architectural role of mitochondrial transcription factor A in maintenance of human mitochondrial DNA. *Mol Cell Biol.* 2004;24(22):9823–9834. https://doi.org/10.1128/MCB.24.22.9823.
21. Ngo HB, Kaiser JT, Chan DC. The mitochondrial transcription and packaging factor Tfam imposes a U-turn on mitochondrial DNA. *Nat Struct Mol Biol.* 2011;18(11):1290–1296. https://doi.org/10.1038/nsmb.2159.
22. Ngo HB, Lovely GA, Phillips R, Chan DC. Distinct structural features of TFAM drive mitochondrial DNA packaging versus transcriptional activation. *Nat Commun.* 2014;5:1–12. https://doi.org/10.1038/ncomms4077.
23. Takamatsu C, Umeda S, Ohsato T, et al. Regulation of mitochondrial D-loops by transcription factor A and single-stranded DNA-binding protein. *EMBO Rep.* 2002;3(5):451–456. https://doi.org/10.1093/embo-reports/kvf099.
24. Hashiya F, Saha A, Kizaki S, Li Y, Sugiyama H. Locating the uracil-5-yl radical formed upon photoirradiation of 5-bromouracil-substituted DNA. *Nucleic Acids Res.* 2014;42(22):13469–13473. https://doi.org/10.1093/nar/gku1133.
25. Watanabe T, Tashiro R, Sugiyama H. Photoreaction at 5′-(G/C)AA^{Br}UT-3′ sequence in duplex DNA: Efficent generation of uracil-5-yl radical by charge transfer. *J Am Chem Soc.* 2007;129(26):8163–8168. https://doi.org/10.1021/ja0692736.
26. Toulme JJ, Charlier M, Helene C. Specific recognition of single-stranded regions in ultraviolet-irradiated and heat-denatured DNA by tryptophan-containing peptides. *Proc Natl Acad Sci USA.* 1974;71(8):3185–3188. https://doi.org/10.1073/pnas.71.8.3185.
27. Behmoaras T, Toulmé JJ, Hélène C. A tryptophan-containing peptide recognizes and cleaves DNA at apurinic sites. *Nature.* 1981;292(5826):858–859. https://doi.org/10.1038/292858a0.
28. Swinger KK, Lemberg KM, Zhang Y, Rice PA. Flexible DNA bending in HU-DNA cocrystal structures. *EMBO J.* 2003;22(14):3749–3760. https://doi.org/10.1093/emboj/cdg351.
29. Yoshida Y, Izumi H, Ise T, et al. Human mitochondrial transcription factor A binds preferentially to oxidatively damaged DNA. *Biochem Biophys Res Commun.* 2002;295(4):945–951. https://doi.org/10.1016/S0006-291X(02)00757-X.
30. Maynard S, Schurman SH, Harboe C, de Souza-Pinto NC, Bohr VA. Base excision repair of oxidative DNA damage and association with cancer and aging. *Carcinogenesis.* 2009;30(1):2–10. https://doi.org/10.1093/carcin/bgn250.
31. Clayton Da, Doda JN, Friedberg EC. The absence of a pyrimidine dimer repair mechanism in mammalian mitochondria. *Proc Natl Acad Sci USA.* 1974;71:2777–2781.
32. Ikeuchi M, Matsusaka H, Kang D, et al. Overexpression of mitochondrial transcription factor A ameliorates mitochondrial deficiencies and cardiac failure after myocardial infarction. *Circulation.* 2005;112(5):683–690. https://doi.org/10.1161/CIRCULATIONAHA.104.524835.